Received: 27 June 2017 | Accepted: 15 December 2017

DOI: 10.1111/jace.15402

ORIGINAL ARTICLE

Journal of the American Ceramic Society

# Thickness-induced anomalous angular-dependent magnetoresistance of $La_{2/3}Sr_{1/3}MnO_3$ thin films grown on $SrTiO_3$

**Xiaotian Li**[1] | **Bin Liu**[1] | **Yiqian Wang**[1] | **Xuyan Xue**[1] | **Guiju Liu**[1] | **Huaiwen Yang**[2] | **Jirong Sun**[2]

[1]College of Physics, Qingdao University, Qingdao, China

[2]Beijing National Laboratory for Condensed Matter Physics, Institute of Physics, Chinese Academy of Sciences, Beijing, China

**Correspondence**
Yiqian Wang, College of Physics, Qingdao University, Qingdao, China.
Email: yqwang@qdu.edu.cn

**Funding information**
National Key Basic Research Development Program of China, Grant/Award Number: 2012CB722705; National Natural Science Foundation of China, Grant/Award Number: 10974105; Program for Foreign Cultural and Educational Experts, Grant/Award Number: GDW20143500163, GDW20163500110; Top-notch Innovative Talent Program of Qingdao City, Grant/Award Number: 13-CX-8

In this paper the effect of thickness on angular-dependent magnetoresistance (MR) of $La_{2/3}Sr_{1/3}MnO_3$ (LSMO) thin films grown on $SrTiO_3$ is systematically investigated. In films thinner than 8 nm, we observe an anomalous weak peak in the MR curves when the magnetic field is parallel to the film surface. In films thicker than 10 nm, however, the weak peak disappears and a novel MR valley appears when the magnetic field is perpendicular to the film surface. The weak peak is thought to be induced by the formation of two-dimensional electron gas (2DEG) at the interface, which is confirmed by density functional theory calculations. The disappearance of the peak and appearance of the valley in the films thicker than 10 nm is associated with the formation of misfit dislocations near the interface between film and substrate, which are clearly visible in high-resolution transmission electron microscopy images. Our work could shed significant light on the influence of film thickness on 2DEG formation.

**KEYWORDS**
dislocations, magnetoresistance, thin films

## 1 | INTRODUCTION

Thin films of the doped perovskite manganites, $La_{1-x}Sr_xMnO_3$, have attracted considerable great attention due to their fascinating physical properties.[1-5] The transport properties of $La_{1-x}Sr_xMnO_3$ films are sensitive to the film thickness and the lattice strain. For example, it was reported that $La_{0.7}Sr_{0.3}MnO_3$ films switched from metallic to insulating when the film thickness was reduced to 2.3 nm.[6] In addition, the effect of quantum interference on the electrical transport properties was observed in $La_{0.9}Sr_{0.1}MnO_3$ films thinner than 4 nm.[7]

Ohtomo and Hwang[8] firstly discovered the conducting two-dimensional electron gas (2DEG) at the interface of 2 insulators, $LaAlO_3$ and $SrTiO_3$ (STO). Recently, the 2DEG has been found at the interface between $La_{0.3}Sr_{0.7}MnO_3$ films and $SrTiO_3$ substrate when the film is thinner than 5 nm, whereas it disappears in the 24-nm films.[9] It is obvious that the film thickness has a substantial effect on the 2DEG. However, the critical film thickness for 2DEG disappearance has not yet been reported. As is well known, the formation of misfit dislocations is closely related to the film thickness. The lattice misfit at the interface can be accommodated by elastic deformation when the epitaxial film is thinner than the critical thickness, while the strain is relaxed via the formation of misfit dislocations when the film thickness exceeds a critical value.[10] The physical properties of perovskite manganite films can be strongly influenced by the formation of misfit dislocations, which

Li and Liu contributed to this work equally.

  

play an important role in the performance of the films.[11,12] Chu et al[13] found that misfit dislocations greatly affect the stability of polarization in ferroelectric perovskites. The electrical transport in the 2DEG can also be influenced by the misfit dislocations since the 2DEG is located at the heterointerface.[14] Many investigations on 2DEG have been reported, both theoretical[15-18] and experimental.[19-21] However, the reason for the disappearance of the 2DEG in the case of thick films is not unveiled. In addition, the direct connection between the misfit dislocations and the properties of LSMO films is still unclear even though the misfit dislocations have been extensively studied in the perovskite manganite films.

In this work we investigate the angular-dependent magnetoresistance (MR) of $La_{2/3}Sr_{1/3}MnO_3/SrTiO_3$ (LSMO/STO) films with a thickness ranging from 6 to 20 nm. When the film is thinner than 8 nm, we find an unexpected weak MR peak with the magnetic field parallel to the film surface. However, when the film is thicker than 10 nm, this peak disappears and an anomalous MR valley is observed with the magnetic field perpendicular to the film surface. The weak MR peak is assigned to a 2DEG formed at the LSMO/STO interface resulting from the magnetic reconstruction, as confirmed by density functional theory calculations. The appearance of the MR valley in films thicker than 10 nm is associated with the formation of misfit dislocations near the interface between film and substrate, which are clearly visible in high-resolution transmission electron microscopy (HRTEM) images. This work could shed light on understanding the influence of film thickness on the 2DEG, and more specifically the reason for the disappearance of the 2DEG in thicker films.

## 2 | EXPERIMENTAL PROCEDURE

$La_{2/3}Sr_{1/3}MnO_3$ films with a thickness of 6, 8, 10, 15, and 20 nm were epitaxially grown on (001) STO substrates (purchased from Hefei Kejing Materials Technology Company) using pulsed laser deposition (PLD) technique. The ceramic target was prepared by a solid-state reaction. During the deposition, the substrates were maintained at 750°C under an oxygen pressure of 50 Pa. The laser wavelength was 248 nm, the pulse fluency was 1.5 J/cm$^2$, and the ablation frequency was 1 Hz. After the deposition, all the films were maintained in an oxygen atmosphere of 30 Pa for 15 minutes and then naturally cooled down to room temperature at 30 Pa. The film thickness is determined from HRTEM images, and the measurement accuracy is about 0.4 nm.

The angular-dependent magnetotransport (MR) measurements were carried out on the physical property measurement system (PPMS, Quantum Design) equipped with sample rotation system using Van Der Pauw method. The MR measurements were performed on the LSMO films with same thickness grown on different STO substrates to make sure that the MR results are reproducible. The silver paste was used as electrical contact in the measurement. During the measurement, the films were clockwise rotated in an applied magnetic field (H = 80 kOe) and the rotation axis was parallel to the sample edge, as shown in Figure 1. The $D_R$ and θ denoted the rotational direction and angle of the film, and the $D_M$ marked the direction of magnetic field. θ = 0° and θ = 90° refer to the magnetic field being perpendicular and parallel to the interface plane, respectively. Two possible current directions, [100] and [010], were considered. As no qualitative difference was found between the 2 in-plane current orientations,[9] the [010] direction was taken in our work.

Specimens for TEM observations were prepared in cross-sectional orientations ([010] zone axis of the STO substrate) using conventional techniques of mechanical polishing and ion thinning. The ion milling was performed using a Gatan Model 691 precision ion polishing system. HRTEM examinations were carried out on a JEOL JEM2100F electron microscope operating at 200 kV. The film structure was analyzed by X-ray diffraction (Bruker X-ray diffractometer, λ = 1.5406 Å). The surface morphology of the films was examined by the atomic force microscope (Seiko SPI 3800N) at the ambient conditions.

The density functional theory (DFT) calculations were implemented in the Cambridge Serial Total Energy Package (CASTEP), including a Hubbard U term accounting for the on-site Coulomb interaction. Exchange-correlation interaction was described by the local density approximation (LDA) with the Ceperley-Alder exchange-correlation potential (CA-PZ) in order to optimize the atomic structures. Spin polarization was taken into account in the

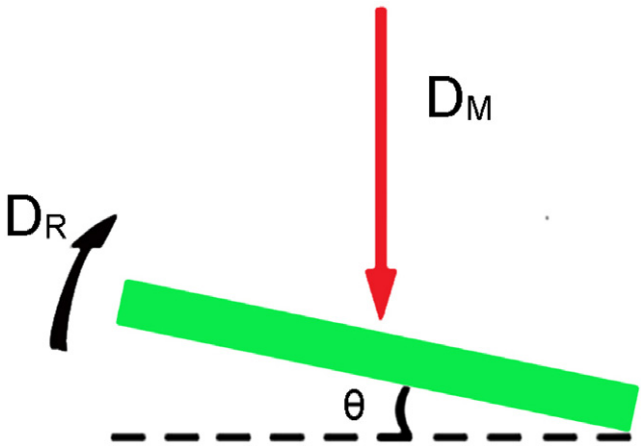


**FIGURE 1** The configuration of angular-dependent magnetotransport measurement [Color figure can be viewed at wileyonlinelibrary.com]

calculations. The calculation was performed using ultrasoft pseudopotential with a 10-eV cut-off energy, and a regular Γ-centered 1 × 1 × 1 k-point mesh in the Brillouin zone.

## 3 | RESULTS AND DISCUSSION

Figure 2 shows the X-ray diffraction (XRD) patterns of the LSMO films with different thickness. In Figure 2, the (002) diffraction peaks of LSMO films and STO substrate can be clearly seen, indicating that all the films are single crystalline and epitaxially grown on the STO substrates. The (002) diffraction peak intensity of LSMO films increases with the thickness of LSMO films. The surface roughness of the LSMO films is examined by the atomic force microscope (AFM) (see Supporting Information). All the films show a step-featured morphology, indicating that their surfaces are relatively flat.

Angular magnetoresistance (MR) is a common feature of ferromagnets due to the anisotropy of spin-dependent scattering. For the ferromagnetic, it is found that the MR depends on the angular θ between the applied magnetic field and the electric current. To investigate the effect of thickness on angular MR, we perform the angular-dependent MR of $La_{2/3}Sr_{1/3}MnO_3/SrTiO_3$ (LSMO/STO) films with a thickness ranging from 6 to 20 nm. The thickness of all the LSMO films is larger than that of the dead layer (3–5 nm) in LSMO.[22] Therefore, the influence of dead layers on the MR measurement is not considered in our work.

Figure 3 shows the angular MR for LSMO/STO films. MR is defined as $R_H/R_0$, where $R_H$ is the resistance at a magnetic field H and $R_0$ is $R_{(H = 0)}$. In the films thinner than 8 nm, 2 different MR peaks are observed. One is observed when the magnetic field is perpendicular to the film surface, which is called out-of-plane MR peak. The out-of-plane peak is the standard resistivity maxima occurring for the ferromagnetic manganites.[23] The other one occurs when the magnetic field is parallel to the film surface, which is called in-plane MR peak (pMR). With the film thickness increasing from 6 to 8 nm, the height of the pMR decreases from 0.00479 to 0.00406. When the film thickness increases to 10 nm, the pMR disappears and an anomalous MR valley (vMR) is observed with the magnetic field perpendicular to the film surface.

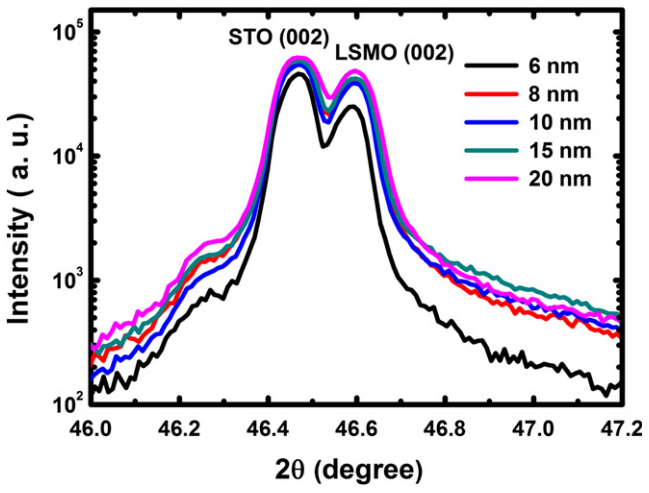


**FIGURE 2** XRD patterns of LSMO films with a thickness of 6, 8, 10, 15, and 20 nm. XRD, X-ray diffraction; LSMO, $La_{2/3}Sr_{1/3}MnO_3$ [Color figure can be viewed at wileyonlinelibrary.com]

Nemes et al[9] believe that the pMR is produced by the 2DEG forming at the LSMO interface. Through DFT calculations, they revealed that the 2DEG arises from the antiferromagnetic coupling (A-type) between a ferromagnetic interfacial manganite layer and the rest LSMO. In their LSMO/STO model used for DFT calculations, La and Sr cations are arranged in order. As we all know, if La and Sr cations are arranged in order, it will be reflected as modulated stripes in the HRTEM images.[24,25] However, in the HRTEM images of LSMO film as shown in Figure 4, no modulated stripes are observed. In other words, the Sr and La cations should be arranged at random in the film. To reconfirm if A-type coupling still exists at the interface of the film when the cations are arranged at random, DFT calculations are also performed in our work. In our LSMO/STO model for the DFT calculations, all the Sr and La cations are arranged at random and the calculated density of states (DOS) is shown in Figure 5. The LSMO is half-metal because its spin-up and spin-down electrons have different nature around the Fermi level. The magnetic moments of Mn cations from the interface to the film surface are calculated to be −3.4, 3.7, and 4.0 $\mu_B$, respectively. It is obvious that the spin polarization of Mn is inverted at the interface. In other words, a manganite layer exists at the interface antiferromagnetically coupling to the rest LSMO. Such a manganite layer would be electrically decoupled as hopping between sites with antiparallel spins is suppressed in half-metals by virtue of double-exchange mechanism,[26] which leads to the formation of 2DEG at the interface and finally gives rise to the appearance of pMR. In our work, the magnetic moments of Mn cations are a little higher than those obtained by Nemes et al as the La and Sr cations are arranged at random in our model.

To explore the influence of different termination layers on the MR, we also carried out the angular-dependent MR measurement of the LSMO films on single-crystalline STO terminated by either SrO or $TiO_2$ (see Supporting Information). From the MR results, it can be seen that the pMR still exists. Therefore, it is believed that the termination layer type of STO substrates does not affect the formation of the 2DEG.

In addition to the pMR, a novel phenomenon is found in our work. When the film is thicker than 10 nm, the

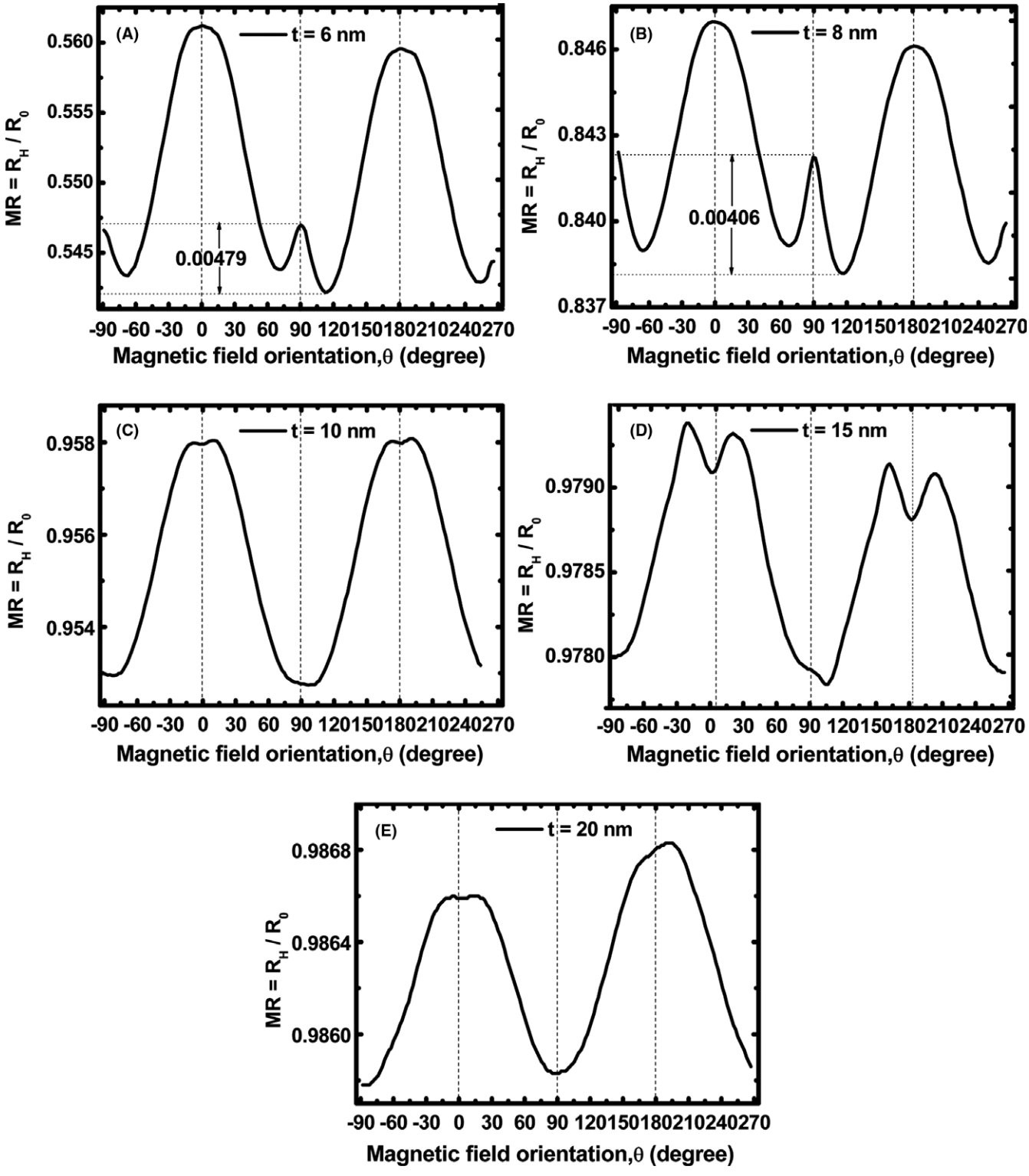


**FIGURE 3** Angular MR for LSMO/STO films with a thickness of 6 nm (A), 8 nm (B), 10 nm (C), 15 nm (D), and 20 nm (E) at 2K, 80 kOe. LSMO/STO, $La_{2/3}Sr_{1/3}MnO_3/SrTiO_3$

pMR disappears and an anomalous vMR is observed with the magnetic field perpendicular to the film surface. In this case, the films are too thick to perform DFT calculations. Considering that the performance of materials depends on their microstructure, we carry out extensive HRTEM examinations of the LSMO/STO interface to clarify the possible reasons for this phenomenon. The typical cross-sectional HRTEM images of 6- and 8-nm-thick LSMO/STO films are shown in the Figures 4 and 6. The interface between film and substrate is marked by dashed lines. No

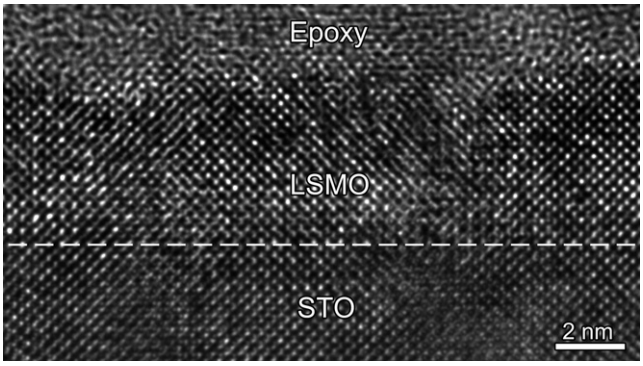


**FIGURE 4** Typical cross-sectional HRTEM image of LSMO/STO with a film thickness of 6 nm. HRTEM, high-resolution transmission electron microscopy; LSMO/STO, $La_{2/3}Sr_{1/3}MnO_3/SrTiO_3$

dislocation can be found near the interface when the film is thinner than 8 nm. However, as the film thickness increases to 10 nm, a pure edge dislocation is observed near the LSMO/STO interface (shown in Figure 7A). To clearly show this dislocation, a magnified HRTEM image of the enclosed rectangle in Figure 7A is shown in Figure 7B. In this image, the extra half atomic plane is clear and the Burgers vector is determined to be <110>. Figure 7C shows the one dimensional Fourier-filtered lattice image of Figure 7B. It is obvious that an extra half plane is vertically inserted. The pure edge dislocation is also observed in the 20-nm-thick LSMO/STO film (shown in Figure 8). According to our HRTEM observations, no misfit dislocation is observed in the 6- and 8-nm-thick films, and no vMR appears. Whereas once the film exceeds 10 nm, the vMR emerged with the appearance of misfit dislocations. Thus, we predict that the disappearance of pMR and the emergence of vMR are associated with the formation of misfit dislocations. To further verify our prediction, the

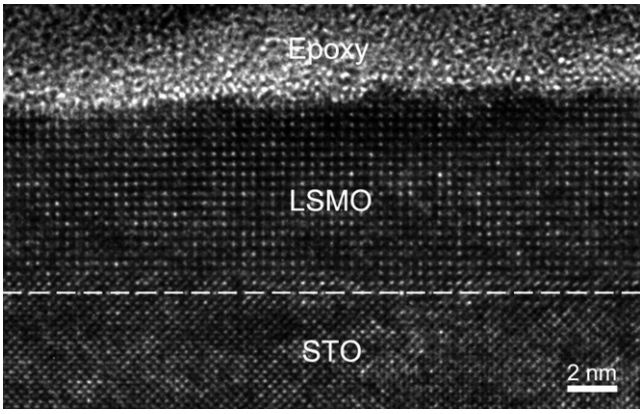


**FIGURE 6** Typical cross-sectional HRTEM image of LSMO/STO with a film thickness of 8 nm. HRTEM, high-resolution transmission electron microscopy; LSMO/STO, $La_{2/3}Sr_{1/3}MnO_3/SrTiO_3$

critical thickness ($t_c$) where a pure edge dislocation existing in the film can be theoretically calculated using the following formula,[27]

$$t_c = \frac{|\vec{b}|}{4\pi f(1+\nu)}\left[\ln\left(\frac{t_c}{|\vec{b}|}\right)+1\right] \quad (1)$$

where $b$ is the Burgers vector ($b \sim 2.736$), $\nu$ is the Poisson ratio ($\nu \sim 0.43$), and $f$ is the lattice mismatch. The lattice mismatch ($f$) can be calculated using the following formula,

$$f = \left(\frac{a_s - a_f}{a_s}\right) \times 100\% \quad (2)$$

where $a_s$ and $a_f$ refer to the lattice parameter of the substrate (3.905 Å) and film (3.87 Å), respectively. $f$ is calculated to be 0.896%. The $t_c$ for the LSMO film is calculated

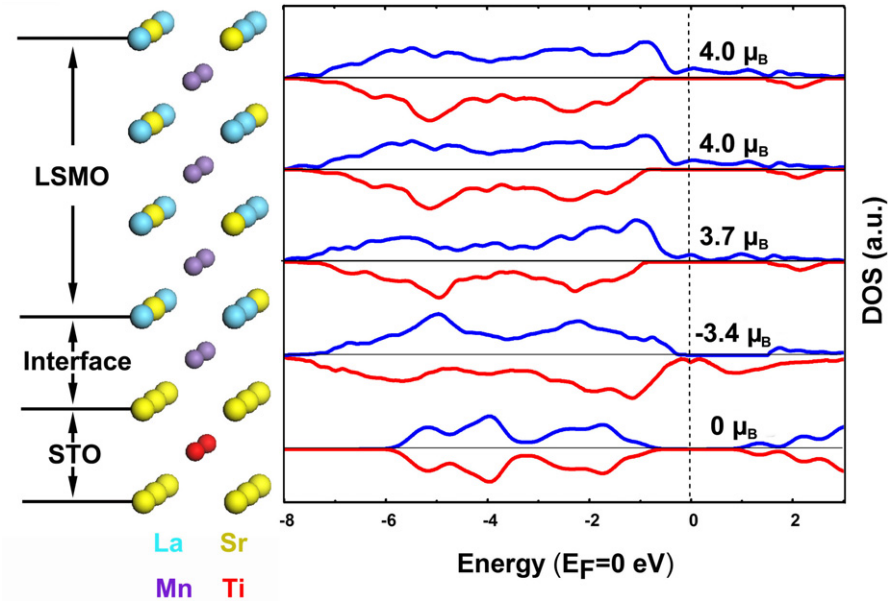


**FIGURE 5** LSMO/STO model (left) for calculation (O atoms are omitted for clarity) and density of states results (right). The dashed line indicates the position of the Fermi level. The upper (blue) and lower (red) lines represent the majority and minority spin densities, respectively. LSMO/STO, $La_{2/3}Sr_{1/3}MnO_3/SrTiO_3$ [Color figure can be viewed at wileyonlinelibrary.com]

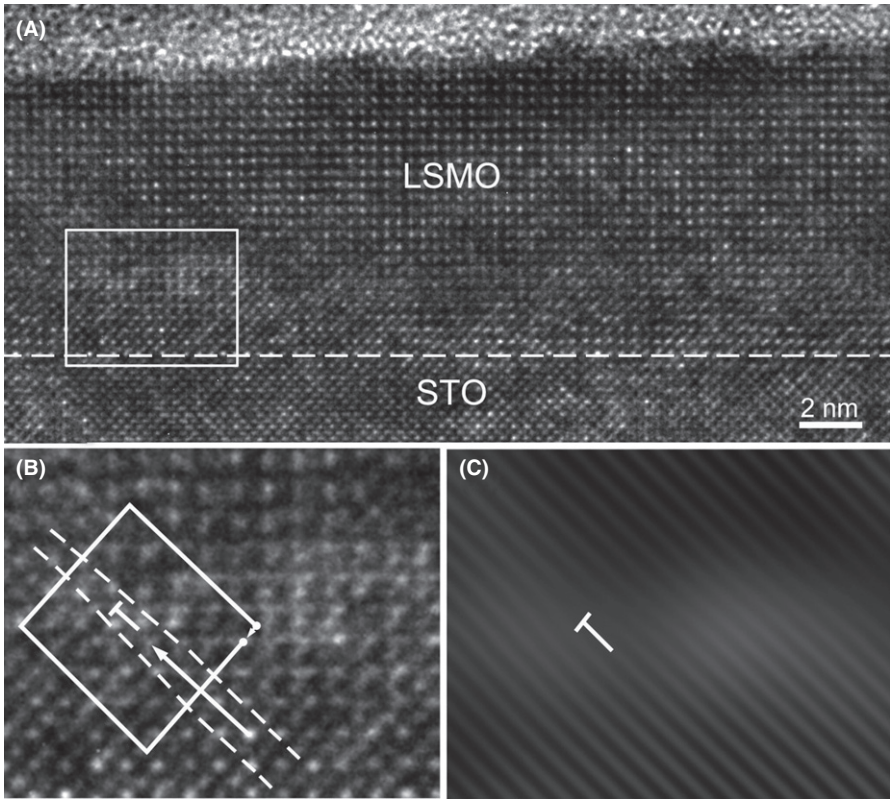


**FIGURE 7** A, Cross-sectional HRTEM image of the LSMO/STO film with a thickness of 10 nm; B, Burgers circuit drawn in enlarged HRTEM image of the region enclosed by a rectangle in (A); C, Fourier filtered lattice image of (B). HRTEM, high-resolution transmission electron microscopy; LSMO/STO, $La_{2/3}Sr_{1/3}MnO_3/SrTiO_3$

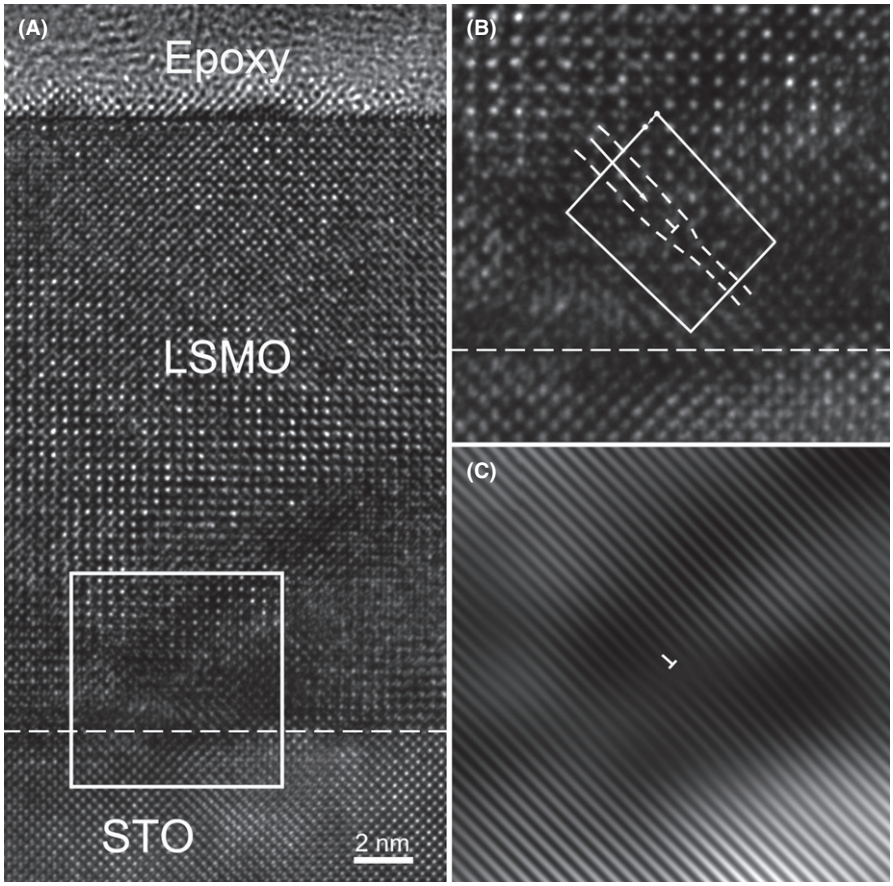


**FIGURE 8** A, Cross-section HRTEM image of the LSMO/STO film with a thickness of 20 nm; B, Burgers circuit drawn in enlarged HRTEM image of the region enclosed by a rectangle in (A); C, Fourier filtered lattice image of (B). HRTEM, high-resolution transmission electron microscopy; LSMO/STO, $La_{2/3}Sr_{1/3}MnO_3/SrTiO_3$

to be 7.27 nm. In other words, the misfit dislocations will form once the film thicker than 7.27 nm. In the Equation (1), the kinetics is ignored. So the actual $t_c$ should be larger than the calculated one and even larger than 8 nm. Thus, no misfit dislocation is formed in the 6- and 8-nm-thick LSMO films. The 2DEG forming at the LSMO interface results in the appearance of pMR. However, when the film thickness exceeds 7.27 nm, the misfit dislocations begin to generate, which could affect the spin polarization at the interface and hinder the magnetic reconstruction. With the increase in the film thickness, the misfit dislocations continue to grow up and the 2DEG gradually disappear. Similar to the previous report,[9] the pMR peak is not prominent with increasing film thickness. When the film thickness increases from 10 to 15 nm, the dominant function in electronic transport at interface gradually changes from 2DEG into misfit dislocation. Consequently the pMR ultimately disappears and the vMR increases. The calculated critical thickness $t_c$ is consistent with our experimental results. Strangely, the vMR becomes indistinct when the film thickness reaches 20 nm. We deduce that the film will gradually possess the property of the bulk materials when it is thick enough. Under this condition, the misfit dislocations have very small impact on the electronic transport at interface and the vMR would become weak and eventually disappeared. That is why the vMR can only be observed in the films that just exceeds the critical thickness.

## 4 | CONCLUSIONS

In summary, we have investigated the effect of film thickness on the angular-dependent MR of thin films grown on STO. When the magnetic field is parallel to the film surface, an additional weak peak appears in the MR curves of the films thinner than 8 nm. As revealed by DFT calculations, this peak signals the formation of 2DEG at the interface which arises from a magnetic reconstruction. However, this 2DEG gradually disappears with increasing film thickness. When the film is thicker than 10 nm, the 2DEG completely disappears and an anomalous vMR simultaneously appears when the magnetic field is perpendicular to the films surface. Combining HRTEM observations and the calculation of critical thickness, we demonstrate that the appearance of this valley is associated with the formation of pure edge dislocations at the interface.

## ACKNOWLEDGMENTS

The authors thank the financial support from the National Key Basic Research Development Program of China (grant no.: 2012CB722705), the National Natural Science Foundation of China (grant no.: 10974105), and the Program for Foreign Cultural and Educational Experts (grant nos.: GDW20143500163, GDW20163500110). Y.Q. Wang thank the financial support from the Top-notch Innovative Talent Program of Qingdao City (grant no.: 13-CX-8), the Taishan Scholar Program of Shandong Province, China, and Qingdao International Center for Semiconductor Photoelectric Nanomaterials.

## ORCID

*Yiqian Wang* http://orcid.org/0000-0002-0538-2541

## REFERENCES

1. Wang LM, Guo CC. Anisotropic magnetoresistance and spin polarization of $La_{0.7}Sr_{0.3}MnO_3/SrTiO_3$ superlattices. *Appl Phys Lett*. 2005;87:172503.
2. Dey P, Nath TK, Taraphder A. Effect of substrate-induced strain on transport and magnetic properties of epitaxial $La_{0.66}Sr_{0.33}MnO_3$ thin films. *Appl Phys Lett*. 2007;91:012511.
3. Yoshimatsu K, Horiba K, Kumigashira H, Ikenaga E, Oshima M. Thickness dependent electronic structure of $La_{0.6}Sr_{0.4}MnO_3$ layer in $SrTiO_3/La_{0.6}Sr_{0.4}MnO_3/SrTiO_3$ heterostructures studied by hard X-ray photoemission spectroscopy. *Appl Phys Lett*. 2009;94:071901.
4. Majumdar S, Huhtinen H, Majumdar HS, Paturi P. Stress and defect induced enhanced low field magnetoresistance and dielectric constant in $La_{0.7}Sr_{0.3}MnO_3$ thin films. *J Alloy Compd*. 2012;512:332-339.
5. Zhou JL, Tra VT, Dong S, et al. Thickness dependence of $La_{0.7}Sr_{0.3}MnO_3/PbZr_{0.2}Ti_{0.8}O_3$ magnetoelectric interfaces. *Appl Phys Lett*. 2015;107:141603.
6. Dorr K, Walter T, Sahana M, et al. Magnetotransport of $La_{0.7}Sr_{0.3}MnO_3/SrTiO_3$ multilayers with ultrathin manganite layers. *J Appl Phys*. 2001;89:6973-6975.
7. Wang C, Jin KJ, Gu L, et al. Magnetoelectric transport and quantum interference effect in ultrathin manganite films. *Appl Phys Lett*. 2014;104:162405.
8. Ohtomo A, Hwang HY. A high-mobility electron gas at the $LaAlO_3/SrTiO_3$ heterointerface. *Nature*. 2004;427:423-426.
9. Nemes NM, Calderón MJ, Beltrán JI, et al. Signatures of a two-dimensional ferromagnetic electron gas at the $La_{0.7}Sr_{0.3}MnO_3/SrTiO_3$ interface arising from orbital reconstruction. *Adv Mater*. 2014;26:7516-7520.
10. Van der Merwe JH. Crystal interfaces part I semi-infinite crystals. *J Appl Phys*. 1963;34:117-122.
11. Gao GY, Jin SW, Wu WB. Lattice-mismatch-strain induced inhomogeneities in epitaxial $La_{0.7}Ca_{0.3}MnO_3$ films. *Appl Phys Lett*. 2007;90:012509.
12. Vailionis A, Boschker H, Liao Z, et al. Symmetry and lattice mismatch induced strain accommodation near and away from correlated perovskite interfaces. *Appl Phys Lett*. 2014;105:131906.
13. Chu MW, Szafraniak I, Scholz R, et al. Impact of misfit dislocations on the polarization instability of epitaxial nanostructured ferroelectric perovskites. *Nat Mater*. 2004;3:87-90.
14. Liu B, Lu YW, Huang Y, Liu GP, Zhu QS, Wang ZG. Interfacial misfit dislocation scattering effect in two-dimensional electron

gas channel of GaN heterojunction. *Phys Lett A*. 2012;376:1067-1071.
15. Popovic ZS, Satpathy S, Martin RM. Origin of the two-dimensional electron gas carrier density at the $LaAlO_3$ on $SrTiO_3$ interface. *Phys Rev Lett*. 2008;101:256801.
16. Li JC, Beltran JI, Munoz MC. Multiorbital structure of the two-dimensional electron gas in $LaAlO_3/SrTiO_3$ heterostructures: the formation of a $d_{xy}$ ferromagnetic sheet. *Phys Rev B*. 2013;87:075411.
17. Zhong ZC, Toth A, Held K. Theory of spin-orbit coupling at $LaAlO_3/SrTiO_3$ interfaces and $SrTiO_3$ surfaces. *Phys Rev B*. 2013;87:161102.
18. Ong PV, Lee J. Orbital-selective charge transfer at oxygen-deficient $LaAlO_3/SrTiO_3$ (001) interface. *Phys Rev B*. 2013;87:195212.
19. Herranz G, Basletic M, Bibes M, et al. High mobility in $LaAlO_3/SrTiO_3$ heterostructures: origin, dimensionality, and perspectives. *Phys Rev Lett*. 2007;9:216803.
20. Kalabukhov A, Gunnarsson R, Borjesson J, Olsson E, Claeson T, Winkler D. Effect of oxygen vacancies in the $SrTiO_3$ substrate on the electrical properties of the $LaAlO_3/SrTiO_3$ interface. *Phys Rev B*. 2007;75:121404.
21. Cen C, Thiel S, Mannhart J, Levy J. Oxide nanoelectronics on demand. *Science*. 2009;323:1026-1030.
22. Angeloni M, Balestrino G, Boggio NG, Medaglia PG, Orgiani P, Tebano A. Suppression of the metal-insulator transition temperature in thin films. *J Appl Phys*. 2004;96:6387-6392.
23. Ben Shalom M, Tai CW, Lereah Y, et al. Anisotropic magnetotransport at the $SrTiO_3/LaAlO_3$ interface. *Phys Rev B*. 2009;80:140403.
24. Liu B, Liu GJ, Feng HL, Wang C, Yang HW, Wang YQ. Effect of oxygen vacancies on structural, electrical and magnetic properties of $La_{0.67}Sr_{0.33}CoO_3$ thin films. *Mater Design*. 2016;89:715-720.
25. Liu B, Wang YQ, Liu GJ, et al. Tuning the magnetic properties of $La_{0.67}Sr_{0.33}CoO_{3-\delta}$ films by oxygen pressure. *Phys Rev B*. 2016;93:094421.
26. Tokura Y. Critical features of colossal magnetoresistive manganites. *Rep Prog Phys*. 2006;69:797-851.
27. People R, Bean JC. Calculation of critical layer thickness versus lattice mismatch for $Ge_xSi_{1-x}/Si$ strained-layer heterostructures. *Appl Phys Lett*. 1985;47:322-324.

## SUPPORTING INFORMATION

Additional Supporting Information may be found online in the supporting information tab for this article.

**How to cite this article:** Li X, Liu B, Wang Y, et al. Thickness-induced anomalous angular-dependent magnetoresistance of $La_{2/3}Sr_{1/3}MnO_3$ thin films grown on $SrTiO_3$. *J Am Ceram Soc*. 2018;101:2339–2346. https://doi.org/10.1111/jace.15402